Electronic Supplementary Material (ESI) for ChemComm.

Supporting Information

Carbon nano-onion induced organization of polyacrylonitrile-derived block star polymers to obtain mesoporous carbon materials

Gabriela Siemiaszko,[1]* Agnieszka Hryniewicka,[1] Joanna Breczko,[1,2] Krzysztof Brzezinski,[3] and Marta E. Plonska-Brzezinska[1]*

1. Department of Organic Chemistry, Faculty of Pharmacy with the Division of Laboratory Medicine, Medical University of Bialystok, Mickiewicza 2A, 15-222 Bialystok, Poland
2. Faculty of Chemistry, University of Bialystok, Ciolkowskiego 1K, 15-245 Bialystok, Poland
3. Department of Structural Biology of Prokaryotic Organisms, Institute of Bioorganic Chemistry, Polish Academy of Sciences, Noskowskiego 12/14, 61-074 Poznan, Poland

E-mail: gsiemiaszko@gmail.com, marta.plonska-brzezinska@umb.edu.pl

MATERIALS AND METHODS

Materials

Commercially available nanodiamond (ND) powder with a crystal size between 4-6 nm (Carbodeon μDiamond®Molto and ND content greater than 97 wt %) was used for the preparation of CNOs. The modified Kuznetsov method for the preparation of CNO by applying an annealing treatment under an inert atmosphere and reduced pressure of ultradispersed ND particles was used.[1,2] CNOs were dried in a furnace at 120 °C overnight before use. *N,N*-Dimethylformamide (DMF, POCH S.A., Poland) was distilled over phosphorus pentoxide (P_2O_5, pure, Honeywell, USA). DMF and acetone (Stanlab, Poland) were dried over 4 Å molecular sieves (POCH S.A., Poland) before use. 2,2'-Azobis(2-methylpropionitrile) (AIBN, ≥95%, POL-AUR, Poland) was recrystallized from methanol (MeOH, Chempur, Poland) before use. 2-MeOH was used as received. Acrylonitrile (≥99%, Aldrich, Germany) was filtered through neutral alumina (Merck, Germany) before use. Ethanesulfonyl azide ($EtSO_2N_3$) was synthesized according to the literature procedure using ethanesulfonyl chloride (≥95%, Aldrich, Germany) and sodium azide (pure, Aldrich, Germany).[3] Potassium dithiobenzoate (KSCSPh) was synthesized from phenylmagnesium bromide 1.0 M solution in THF (Merck, Germany) and carbon disulfide 5.0 M solution in THF (Merck, Germany) using adapted literature procedure.[4] The glassware and potassium bromide (KBr, ≥99%, Aldrich, Germany) were dried in a furnace at 120 °C overnight before use. Deuterated solvent, dimethylsulfoxide (DMSO-d_6), was purchased from Euroisotop (United Kingdom). In electrochemical measurements, aqueous solutions of sodium hydroxide (NaOH, 97%, Aldrich, Germany), sulfuric acid (H_2SO_4, 95%, Chempur, Poland), and sodium sulfate (Na_2SO_4, Chempur, Poland) were used.

Methods

High-resolution transmission electron microscopy (HRTEM) was performed using a Titan G2 HRTEM microscope (FEI Company) equipped with a field emission gun (FEG). Electron beam accelerating voltage was 300 kV. HRTEM imaging of the sample microstructure was performed in bright field mode using a CCD camera as a detector. Before analysis, the samples were ground in an agate mortar to a fine powder. Into the obtained powder, 99.8% ethanol (POCH, Poland) was poured to form a suspension, which was placed in an ultrasonic homogenizer for 10 seconds. The resulting slurry was taken with a pipette, placed on copper grids (200

mesh/inch) coated with carbon-stabilized formvar (Ted Pella, USA), and left for ethanol to evaporate.

The SEM measurements were performed using an INSPECT S50 microscope (FEI, Japan). The accelerating voltage of the electron beam was 15 keV. Before the measurements, a gold layer with a thickness of 7 nm was sputtered on the surface of the analyzed samples.

X-ray photoelectron spectroscopy (XPS) was performed using an ultrahigh vacuum chamber (PREVAC) with base pressure below 10−8 mbar using an Al Kα nonmonochromatic radiation source (1486.7 eV; 12 kV; 12 mA; VG Scienta SAX 100) and monochromator (VG Scienta XM 780). Detection of emitted photoelectrons was performed using a Scienta R4000 hemispherical analyzer. A low-resolution survey run (0-1200 eV) at a pass energy of 200 eV was carried out. The C 1s, O 1s, and N 1s high-resolution spectra were recorded at a pass energy of 50 eV at room temperature. All the spectra were fitted by Shirley background subtraction before Gaussian-Lorentzian functions using CasaXPS software (Casa Software Ltd.).

For X-ray powder diffraction (XRD) measurements, the samples were loaded into glass capillaries (Hampton Research, Glass Number 50) with a diameter of 0.5 mm. The X-ray powder diffraction data were measured using CuKα radiation at 298 K on XtalLAB Synergy diffractometer (Rigaku) equipped with the Hybrid Pixel 2-dimensional detector HyPix-6000HE. For all experiments, the sample-to-detector distance was set to 148 mm, and the data were recorded for the 2θ angle ranging from 10° to 100° using the standard phi scan procedure. In all experiments, the exposure time was 60 seconds.

The room-temperature Raman spectra were taken with a Renishaw inVia confocal spectrometer (United Kingdom). The parameters used for the Raman measurements were as follows: laser with a wavelength of 785 nm (2.33 eV), power of the laser beam of 2 mW, and a spectral resolution of 2 cm^{-1}. The spectra obtained after normalization were analyzed using OMNIC spectroscopy software.

Fourier transform infrared spectroscopy (FTIR) was performed using a Thermo Scientific Nicolet IN10 MX microscope (USA). The spectra were recorded in a KBr pellet using a microscope in transmission mode. The spectra were collected with a resolution of 4 cm^{-1}, and 64 scans were averaged to obtain a single spectrum.

^{1}H spectra were recorded on an Agilent VNMRS system operated at 500 MHz. Chemical shifts δ are given in ppm, referenced to the solvent peak of DMSO-d_6, defined at δ = 2.50. The

following abbreviations were used for multiplicities: s (singlet), d (doublet), t (triplet), q (quartet), m (multiplet).

Size exclusion chromatography (SEC) was performed using high-performance liquid chromatography (Merck-Hitachi, Germany) equipped with a Phenogel Linear chromatography columns, 5 µm, 300 mm × 7.8 mm (Merck, Germany) and PLgel 5µm, 100Å, 300 x 7,8 mm (Agilent, USA). Detector UV-VIS/DAD 7450A (wavelength 278 nm) was used. A mixture of narrowly dispersive polystyrene molecular weight standards of molecular weight from 1 000 000 Da to 500 Da (Merck, Germany) was used to calibrate the molecular weight distribution. The sample was analyzed at a concentration of 2.5 mg mL^{-1} in DMF (Sigma Aldrich, Germany). The separation process was carried out at 55 °C with a mobile phase volume flow (DMF) of 1.0 mL min^{-1}. The volume of the dosed sample was 50 µL.

Samples were pyrolyzed using a Carbolite Gero STF 16/180 + 3216 Controller tube furnace.

Voltammetric studies were performed using a PGSTAT 302N potentiostat (Autolab B.V., Metrohm, Utrecht, the Netherlands) with a three-electrode system (glassy carbon electrode (GCE, Ø 2 mm) as the working electrode, Ag/AgCl as the reference electrode and Pt mesh (0.25 mm) as the counter electrode). Before the measurements, the surface of the GCE was polished with carborundum paper and modified by using 15 µL of the synthesized material solution (3 mg mL^{-1} in EtOH) with the addition of conductive carbon paint (CP, SPI Supplies, USA). Then the solvent was evaporated at RT under an Ar atmosphere. The addition of CP was intended to improve the mechanical stability of the film formed on the electrode surface. All measurements were carried out in 1 M aqueous solutions of NaOH, H_2SO_4, and Na_2SO_4.

EXPERIMENTAL PROCEDURES

General procedure of synthesis of 6-*star*-(PMA-*b*-PAN) polymers (P1-P4)

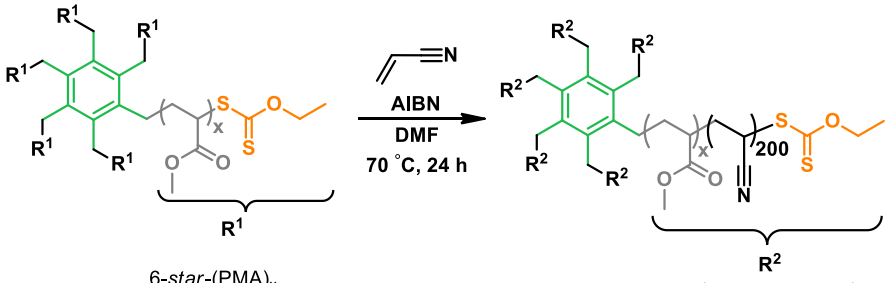

6-*star*-$(PMA)_x$
x = 25, 50, 100, 150

6-*star*-$(PMA_x$-*b*-$PAN_{200})$
P1, x = 25
P2, x = 50
P3, x = 100
P4, x = 150

The 6-*star*-(PMA) polymer (synthesized previously),[5] acrylonitrile, and AIBN were dissolved in DMF. Argon was bubbled through for 15 min. The reaction mixture was stirred for 24 h at 70 °C under argon. The polymers were then precipitated with MeOH, followed by filtration and drying on a vacuum pump, affording the products as pale orange to white powders. Synthetic details are given in the table below. **P4**: ^{1}H NMR (DMSO-d_6, 500 MHz) characteristic signals: δ 4.61 (q, J = 7.1 Hz, 2H, -CH_2CH$_3$), 3.57 (s, -OCH_3), 3.25-3.00 (m, -CH$_2$CHCN), 2.35-1.95 (m, -CH$_2$CHC(O)-, -CH_2CHCN), 1.85-1.35 (m, CH_2CHC(O)-).

Product	6-*star*-(PMA)				Acrylonitrile				AIBN			DMF (mL)	Product (g)
	Substrate	$M_{n,\,th}$ (g mol^{-1})	equiv	n (mmol)	m (g)	equiv	n (mmol)	V (mL)	equiv	n (mmol)	m (mg)		
P1	6-*star*-(PMA_{25})	13796.9	1.0	0.039	0.534	1200	46.43	3.04	1.98	0.077	12.6	7.39	2.15
P2	6-*star*-(PMA_{50})	26710.4	1.0	0.033	0.884	1200	39.73	2.60	1.98	0.066	10.8	6.32	2.34
P3	6-*star*-(PMA_{100})	52537.4	1.0	0.026	1.350	1200	30.83	2.02	1.98	0.051	8.35	4.91	2.37
P4	6-*star*-(PMA_{150})	78364.4	1.0	0.021	1.645	1200	25.19	1.65	1.98	0.042	6.82	4.01	2.00

Synthesis of PAN- and CNO-based hybrid materials

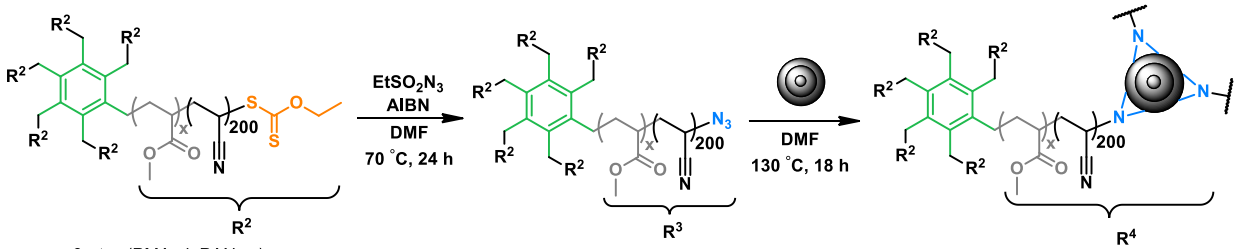

Synthesis of 6-star-(PMA$_{150}$-b-PAN$_{200}$-N$_3$) polymers (P1-N$_3$, P4-N$_3$)

The polymer **P1** or **P4**, $EtSO_2N_3$, and AIBN (equal portion added every 1 h) were dissolved in anhydrous DMF and the reaction mixture was stirred for 24 h at 70 ˚C. The polymer was then precipitated with MeOH, followed by filtration and drying on a vacuum pump, affording the product as a white powder. Synthetic details are given in the table below. **P4-N$_3$**: ^{1}H NMR (DMSO-d_6, 500 MHz) characteristic signals: δ 3.57 (s, -OCH_3), 3.25-3.00 (m, -CH$_2$CHCN), 2.35-1.95 (m, -CH$_2$CHC(O)-, -CH_2CHCN), 1.85-1.35 (m, CH_2CHC(O)-).

Product	6-*star*-(PMA-*b*-PAN)					$EtSO_2N_3$				AIBN			DMF (mL)	Product (g)
	Substrate	$M_{n,\,th}$ (g mol^{-1})	equiv	n (mmol)	m (g)	n (mmol)	equiv	n (mmol)	m (mg)	equiv	n (mmol)	m (mg)		
P1-N$_3$	P1	77468.9	1.0	0.0090	0.7	0.0090	151	1.36	183.14	24.0	0.22	35.61	2.80	0.737
P4-N$_3$	P4	142036.4	1.0	0.0049	0.7	0.0049	151	0.74	99.89	24.0	0.12	19.42	2.80	0.699

Synthesis of 6-star-(PMA$_{150}$-b-PAN$_{200}$)-CNO polymer-carbon hybrids (P1-CNO, P4-CNO)

The **P1-N$_3$** or **P4-N$_3$** polymer and CNOs in anhydrous DMF were stirred for 18 h at 130 ˚C under argon. The resulting reaction mixture was precipitated with MeOH, followed by drying on a vacuum pump, affording a product as a black powder. Synthetic details are given in the table below.

Product	6-*star*-(PMA-*b*-PAN-N$_3$)		CNO	DMF (mL)	Product (g)
	Substrate	m (g)	m (mg)		
P1-CNO	P1-N$_3$	0.400	10.0	10.0	0.325
P4-CNO	P4-N$_3$	0.570	10.0	10.0	0.482

Synthesis of polymer derived from CNO-derived dithiocarbonate

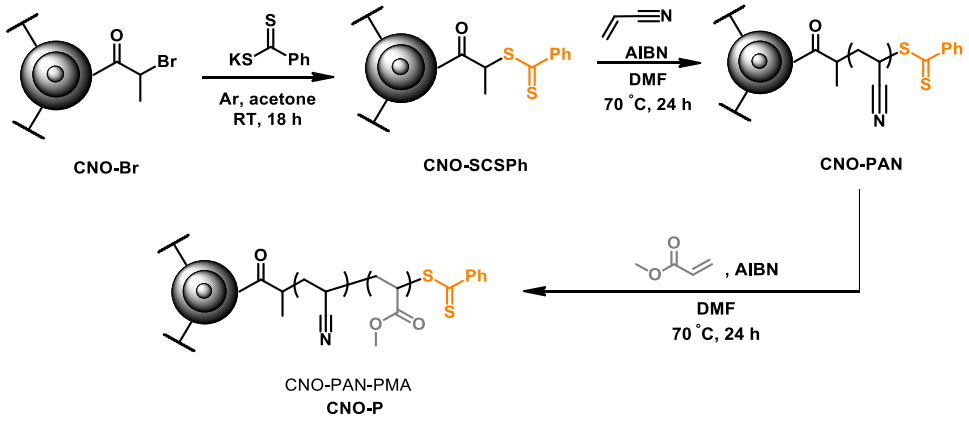

Synthesis of CNO-derived dithiocarbonate (CNO-SCSPh)

2-Bromopropionyl-CNOs obtained previously[5] (CNO-Br, 20.0 mg) were suspended in anhydrous acetone (10.0 mL) under Ar and sonicated for 30 min. KSC(S)Ph (0.10 mol, 0.20 g) was added and the reaction mixture was stirred for 18 h at room temperature. Then the functionalized CNOs were filtered off, washed with acetone, and methanol, followed by drying in vacuo affording 24.0 mg of the products as black powders.

Synthesis of CNO-PAN

CNO-SCSPh (7 mg) was suspended in a solution of AIBN (0.033 mmol, 5.4 mg) and acrylonitrile (18.78 mmol, 1.23 mL) anhydrous DMF (4.0 mL). Argon was bubbled through this suspension for 15 min., followed by sonification for 30 min. Next, the reaction mixture was stirred for 24 h at 70 °C. After cooling, the polymer was precipitated to MeOH affording 420 mg of the product as a black powder.

Synthesis of CNO-P

CNO-PAN was suspended in a solution of AIBN (0.012 mmol, 2.0 mg) and methyl acrylate (5.8 mmol, 0.53 mL) in DMF (3.0 mL). Argon was bubbled through this suspension for 15 min., followed by sonification for 30 min. Next, the reaction mixture was stirred for 24 h at 70 °C. After cooling, the polymer was precipitated to MeOH affording 640 mg of the product as a grey-green powder.

Thermal treatment

Stabilization

All the PAN-derived polymers and hybrids were heated to 250 °C with a ramping rate equal to 2 °C min^{-1}, followed by stabilization for 4 h at 250 °C with constant air flow. Next, the samples were cooled down to room temperature with a ramping rate equal to 10 °C min^{-1} with constant argon flow.

Pyrolysis

The PAN-derived stabilized materials were heated to 800 °C with a ramping rate equal to 5 °C min^{-1} and pyrolyzed for 2 h at 800 ˚C with constant argon flow. Next, the samples were cooled down to room temperature with a ramping rate equal to 10 °C min^{-1} with constant argon flow.

TABLES AND FIGURES

Table S1. Summary of molecular weights and dispersity indexes obtained from ^{1}H NMR and SEC analyses.

Polymer	Polymer composition	$M_{n,\,th}$ [a]	$M_{n,\,NMR}$ [b]	wt% PMA [c]	$M_{n,\,SEC}$ [d]	Đ [d]
P1	6-*star*-(PMA$_{25}$-*b*-PAN$_{200}$)	77 469	130 346	15.2	87 838	2.69
P2	6-*star*-(PMA$_{50}$-*b*-PAN$_{200}$)	90 382	141 902	25.3	115 794	2.68
P3	6-*star*-(PMA$_{100}$-*b*-PAN$_{200}$)	116 209	160 274	44.1	121 328	2.91
P4	6-*star*-(PMA$_{150}$-*b*-PAN$_{200}$)	142 036	175 913	54.9	127 193	2.95

[a] $M_{n,\,th} = M_{CTA} + M_{MA} \cdot equiv_{MA} + M_{AN} \cdot equiv_{AN}$; the degree of monomer conversion was not considered. [b] $M_{n,\,NMR} = M_{CTA} + (M_{MA} \cdot x_{MA} + M_{AN} \cdot x_{AN}) \cdot 6$; x_{MA} is integrated signal taken from ^{1}H NMR spectrum corresponding to singlet from 3H of -CH_3 group (PMA repeating unit) at ca. 3.57 ppm, while x_{AN} corresponds to integrated multiplet at ca. 3.15 ppm from 1H of -C*H*CN, compared to a quartet of 2H of -CH_2- at 4.63 ppm. [c] wt % PMA = $(M_{MA} \cdot x_{MA}) : (M_{MA} \cdot x_{MA} + M_{AN} \cdot x_{AN})$. [d] Measured by SEC.

Table S2. Summary of PAN-derived carbon materials.

Stabilization and pyrolysis substrate	Stabilization product	Pyrolysis product	wt% stabilization [a]	wt% pyrolysis [b]	wt% CNO [c]
P1	**P1-S**	**P1-C**	84%	50%	-
P2	**P2-S**	**P2-C**	82%	46%	-
P3	**P3-S**	**P3-C**	84%	38%	-
P4	**P4-S**	**P4-C**	79%	35%	-
P1-CNO	**P1-CNO-S**	**P1-CNO-C**	83%	55%	5.2%
P4-CNO	**P4-CNO-S**	**P4-CNO-C**	74%	34%	6.1%
CNO-P	**CNO-P-S**	**CNO-P-C**	88%	53%	2.0%

[a] wt% stabilization= $(m_S : m_P) \cdot 100\%$, where m_S is the mass of the sample obtained by stabilization, m_P is mass of the polymeric sample. [b] wt% pyrolysis= $(m_C : m_P) \cdot 100\%$, where m_c is mass of the sample obtained by pyrolysis, m_P is mass of the polymeric sample. [c] wt% CNO = $(m_{CNO} : m_C) \cdot 100\%$, where m_{CNO} is the mass of CNOs subjected to the synthesis, m_C is the mass of carbon material. The lines of the table represent the corresponding samples and should be interpreted as follows: the "Stabilisation and pyrolysis substrate" was the substrate to give a "Stabilization product", which after pyrolysis afforded "Pyrolysis product".

Table S3. Surface Elemental Composition of selected carbon samples determined by XPS.

Sample	Elements (%)		
	C	**N**	**O**
P1-C	84.20	7.30	8.51
P4-C	89.78	6.71	3.51
P1-CNO-C	89.60	6.08	4.32
P4-CNO-C	86.62	8.00	5.39
CNO-P	86.78	4.46	8.76

Table S4. Distribution of elements obtained from the deconvolution of the C 1s, O 1s, and N 1s spectra by XPS of **P1-C**, **P4-C**, **P1-CNO-C**, **P4-CNO-C**, and **CNO-P-C** materials.

Region	Peak	BE (eV)	Assignment	References	Concentration (%)				
					P1-C	**P4-C**	**P1-CNO-C**	**P4-CNO-C**	**CNO-P-C**
C 1s	**A**	285.0 ± 0.1	C-H sp^3	[6]	19.0	18.8	17.0	18.5	19.3
	B	284.4 ± 0.1	C=C sp^2	[6,7]	37.5	39.1	43.9	39.5	37.4
	C	285.6 ± 0.1	C-C sp^3	[6,7]	11.2	11.7	10.5	11.7	13.0
	D	286.4 ± 0.1	C-OH, C-N (aziridine)	[6–8]	7.9	7.8	6.8	7.6	7.6
	E	287.1 ± 0.1	C-O-C	[6,7]	3.0	2.7	3.2	3.5	3.0
	F	287.8 ± 0.1	C=O	[6,7]	2.4	2.5	2.3	2.4	1.6
	G	288.6 ± 0.1	O=C-O-	[7,9]	4.0	1.8	1.7	2.2	2.7
	H	289.5 ± 0.1	O=C-OH	[9]	1.5	1.6	1.7	1.6	2.7
	I	290.8 ± 0.1	π-π*	[10]	1.1	1.4	1.5	0.9	0.8
	DCS 1	283.9 ± 0.1	defects in the carbon structure	[11,12]	9.9	9.9	8.7	10.4	9.8
	DCS 2	283.4 ± 0.1	defects in the carbon structure	[11,12]	2.5	2.6	2.7	1.8	2.4
N 1s	**A**	398.0 ± 0.1	pyridinic-N	[13,14]	39.9	34.3	36.6	41.2	37.9
	B	400.0 ± 0.1	pyrrolic-N	[8,15–17]	16.3	17.5	18.4	19.7	15.5
	C	400.7 ± 0.1	quaternary N	[13,14]	35.8	40.6	34.1	31.8	35.5
	D	403.0 ± 0.1	N-oxides of pyridinic-N	[13,14]	8.0	7.6	11.0	7.3	11.1
O 1s	**A**	530.6 ± 0.2	quinones	[18]	5.7	20.6	26.9	30.8	7.6
	B	532.1 ± 0.2	C=O, O=C-O, C-O	[18,19]	52.6	43.6	44.0	43.8	51.4
	C	533.4 ± 0.2	Ar-OH, Ar-COO-, C-O-C	[18,20]	39.8	25.3	19.9	19.6	38.9
	D	535.0 ± 0.3	adsorbed oxygen or water	[18,21]	2.0	10.5	9.2	5.8	2.1

Table S5. Textural parameters from the N_2 adsorption/desorption analysis.

Sample	BET surface area[1] ($m^2\ g^{-1}$)	Micropore surface area[2] ($m^2\ g^{-1}$)	Mesopore surface area[2] ($m^2\ g^{-1}$)	Pore volume[3] ($cm^3\ g^{-1}$)	Pore size[4] (nm)
P1-C	1	0.8	0.2	0.0024	9
P2-C	10	5	5	0.0262	10
P3-C	19	5	14	0.0669	12
P4	2	0	2	0.0022	4
P4-S	6	0	6	0.0024	2
P4-C	28	11	17	0.0863	13
P1-CNO-C	31	13	18	0.0704	9
P4-CNO-C	74	5	69	0.2364	13
CNO	414	0	414	1.4384	14
CNO-P-C	29	18	11	0.0255	3

[1] Surface area calculated based on Brunauer-Emmett-Teller (BET) isotherm;

[2] Micropore and mesopore surface areas calculated based on t-plot analysis;

[3] Pore volume calculated based on BJH adsorption cumulative volume of pores between 17.000 Å and 3000.000 Å diameter;

[4] Pore size calculated based on adsorption average pore width (4V/A by BET).

Table S6. Specific capacitances of the synthesized materials calculated from the integration of i_c vs. E (from -0.6 to 0 V).

Sample	Specific capacitance ($F\ g^{-1}$)
P1-C	5
P2-C	14
P3-C	39
P4-C	45
P1-CNO-C	53
P4-CNO-C	83
CNO	23
CNO-P-C	24

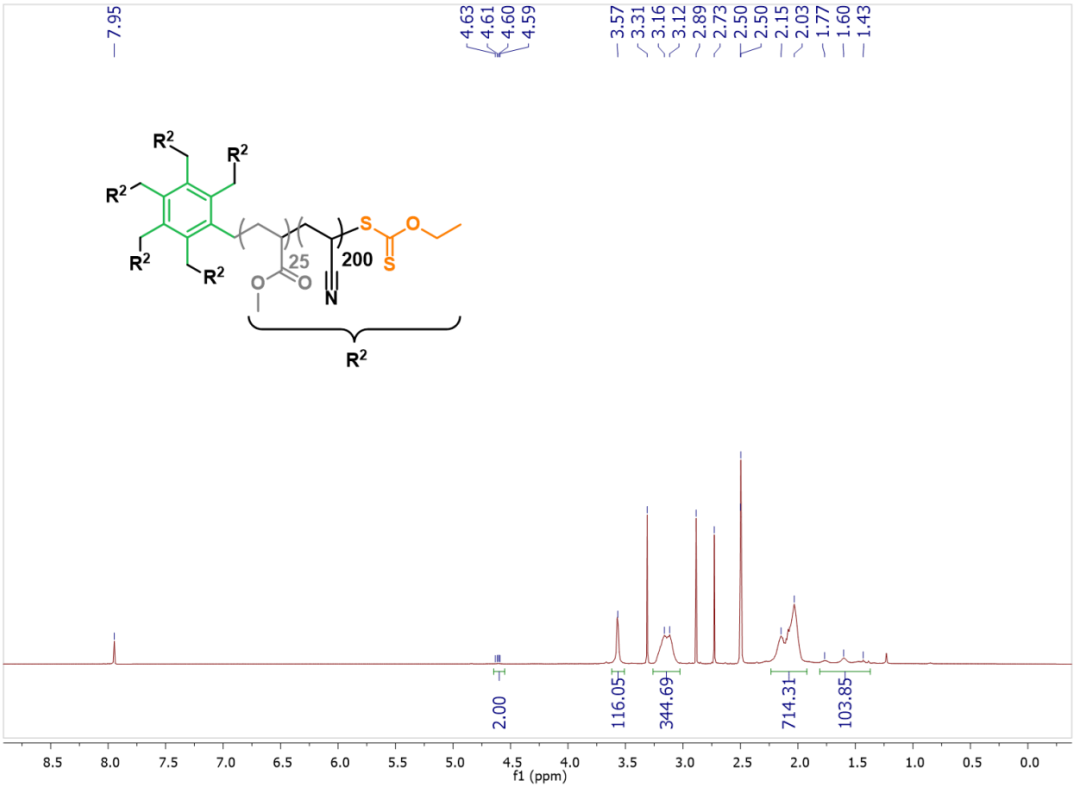

Figure S1. ^{1}H NMR spectrum of 6-*star*-(PMA$_{25}$-*b*-PAN$_{200}$) (**P1**) polymer.

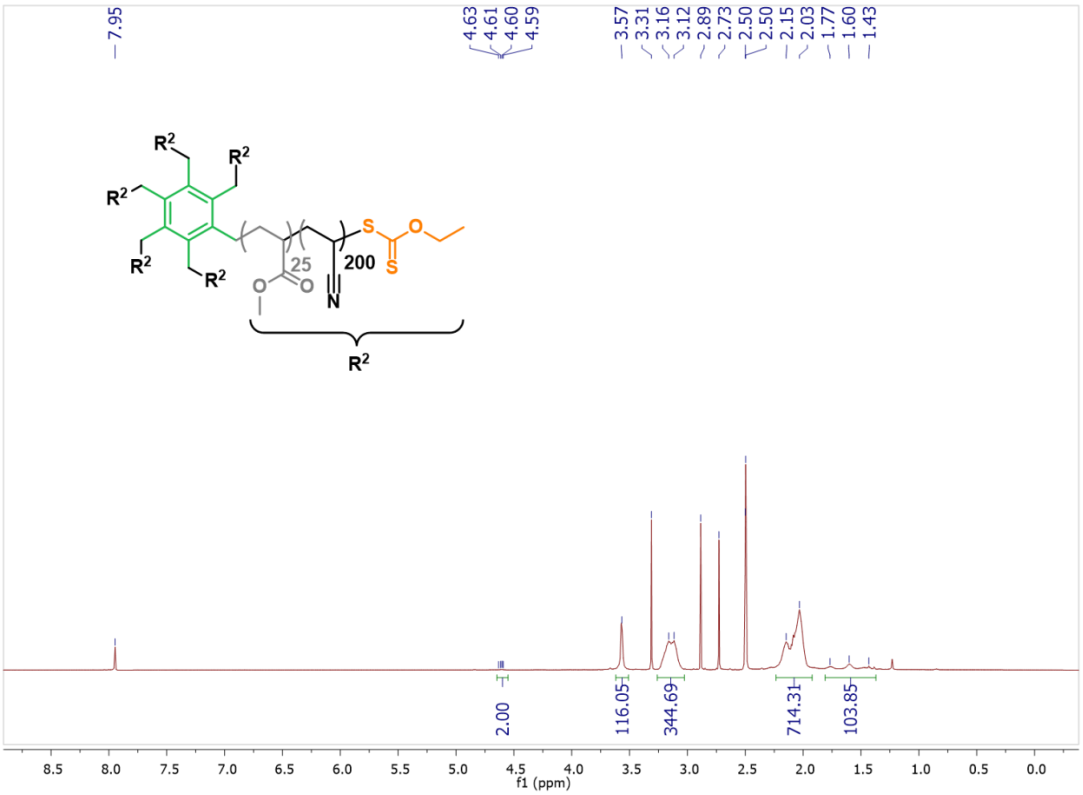

Figure S2. ^{1}H NMR spectrum of 6-*star*-(PMA$_{50}$-*b*-PAN$_{200}$) (**P2**) polymer.

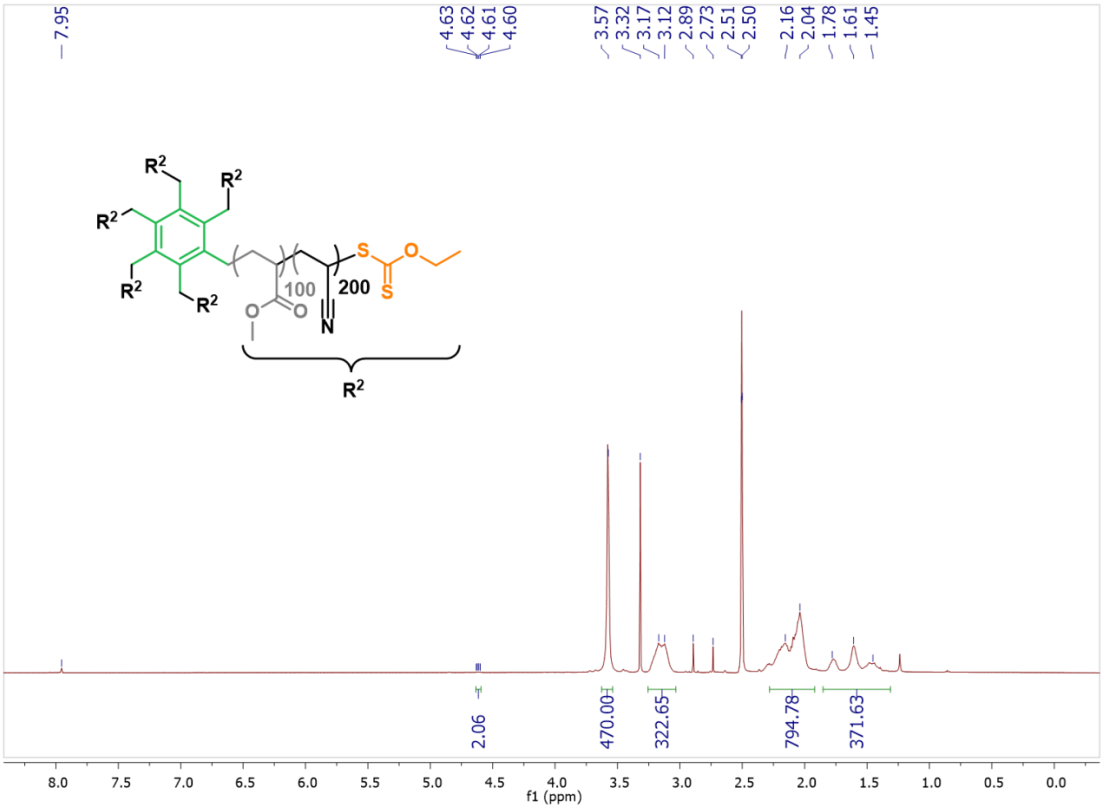

Figure S3. ^{1}H NMR spectrum of 6-*star*-(PMA$_{50}$-*b*-PAN$_{200}$) (**P3**) polymer.

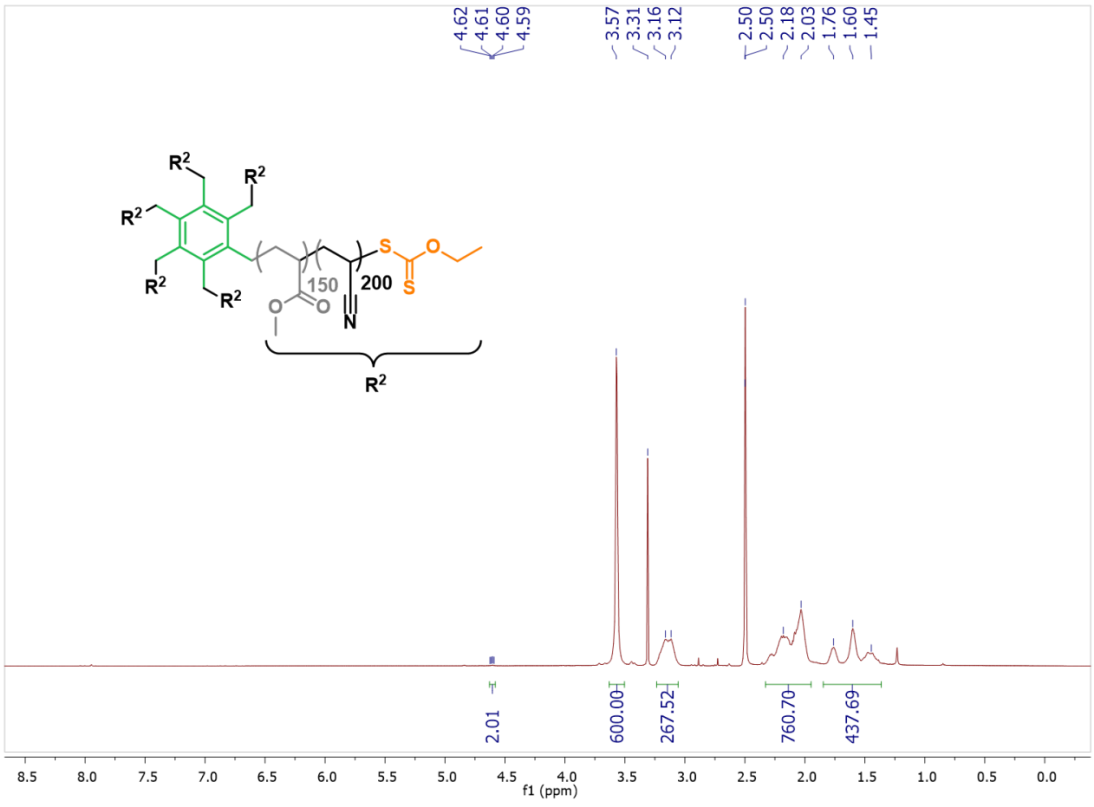

Figure S4. ^{1}H NMR spectrum of 6-*star*-(PMA$_{150}$-*b*-PAN$_{200}$) (**P4**) polymer.

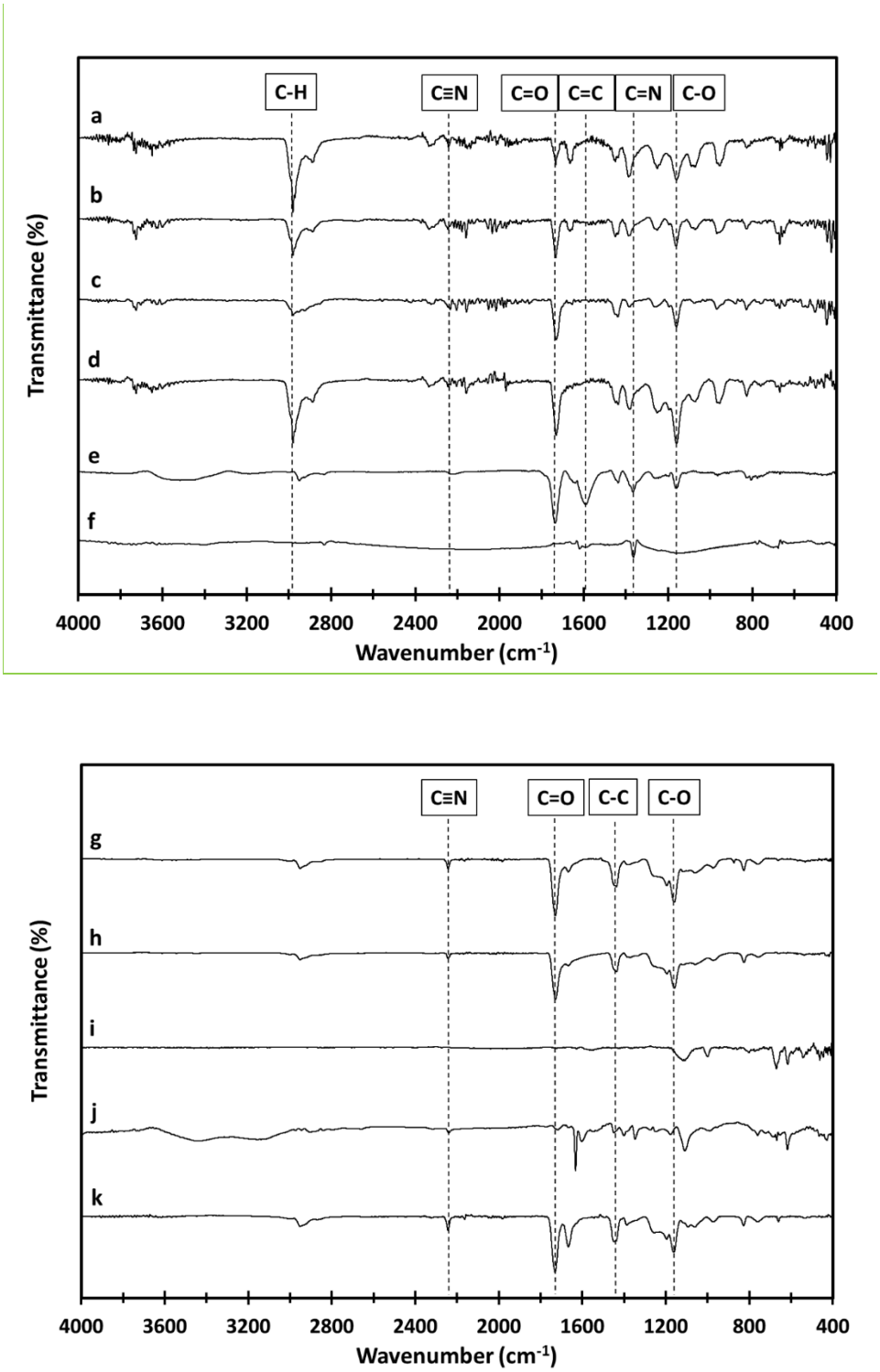

Figure S5. FT-IR spectra of (a) **P1**, (b) **P2**, (c) **P3**, (d) **P4**, (e) **P4-S**, (f) **P4-C**, (g) **P4-N_3**, (h) **P4-CNO**, (i) **CNO-SCSPh**, (j) **CNO-PAN**, (k) **CNO-P**.

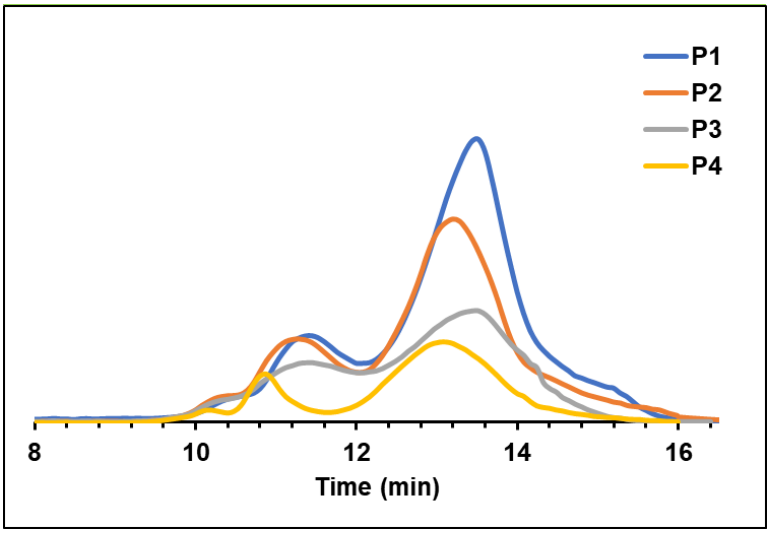

Figure S6. SEC traces of **P1**, **P2**, **P3**, and **P4**.

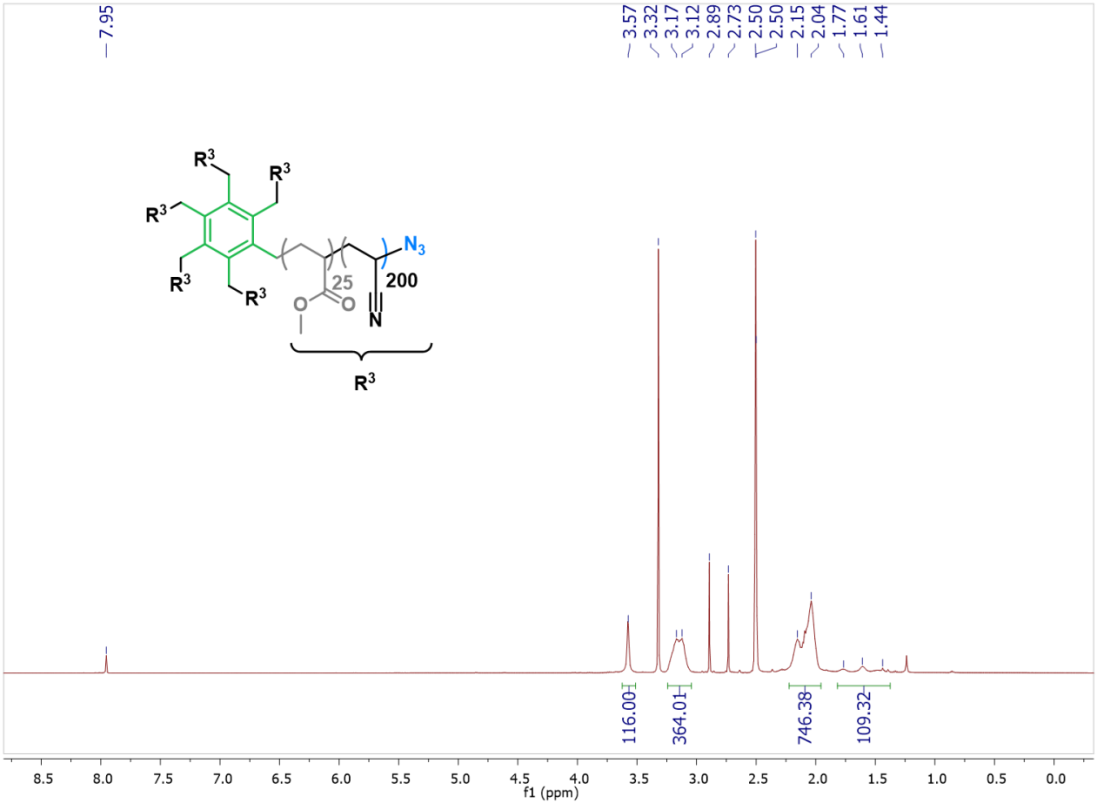

Figure S7. ^{1}H NMR spectrum of 6-*star*-(PMA$_{25}$-*b*-PAN$_{200}$-N$_3$) (**P1-N$_3$**) polymer.

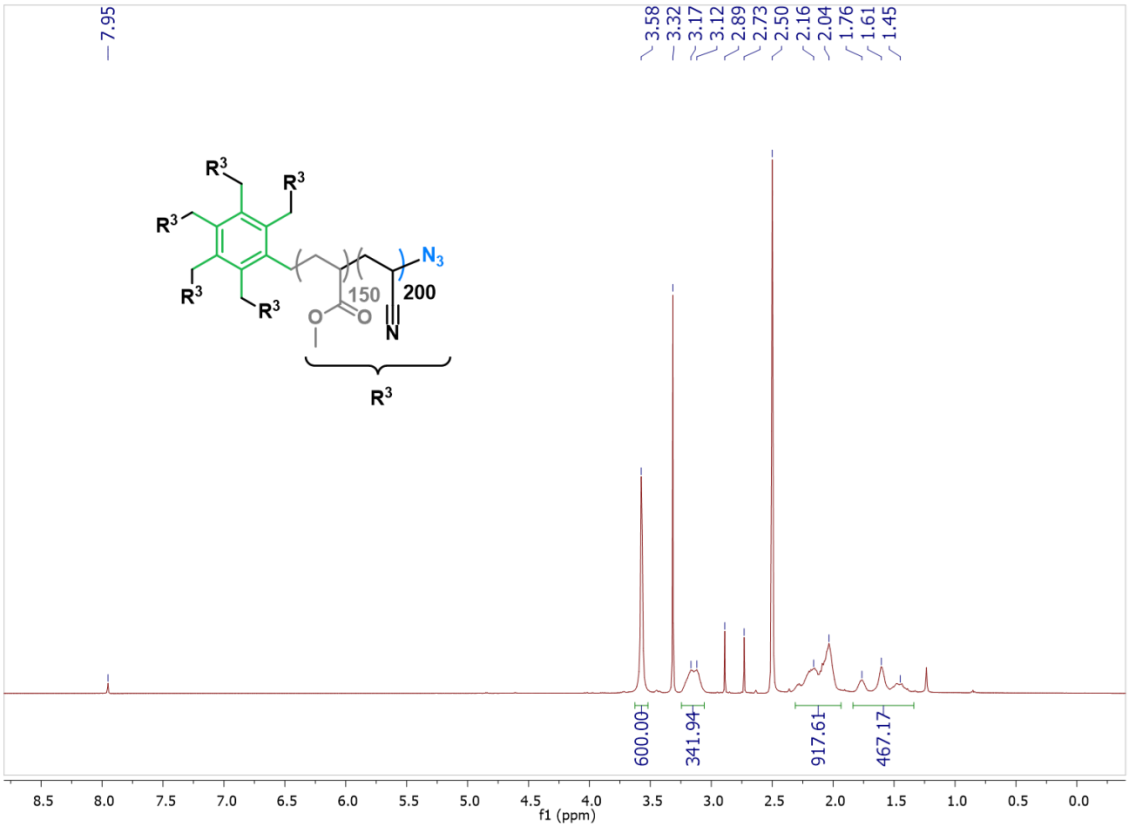

Figure S8. ^{1}H NMR spectrum of 6-*star*-(PMA$_{150}$-*b*-PAN$_{200}$-N$_3$) (**P4-N$_3$**) polymer.

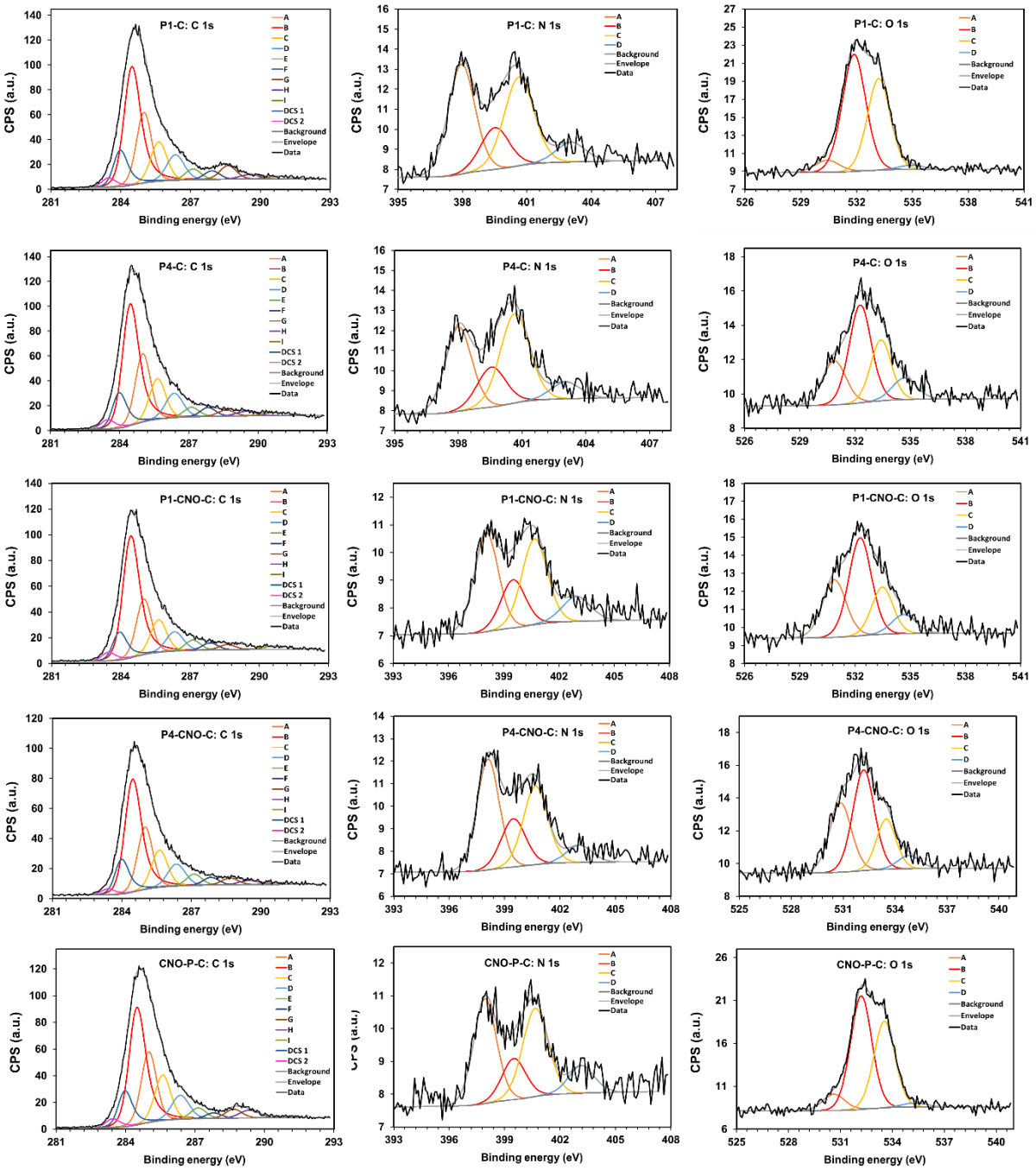

Figure S9. XPS deconvolution spectra of **P1-C**, **P4-C**, **P1-CNO-C**, **P4-CNO-C**, and **CNO-P-C**.

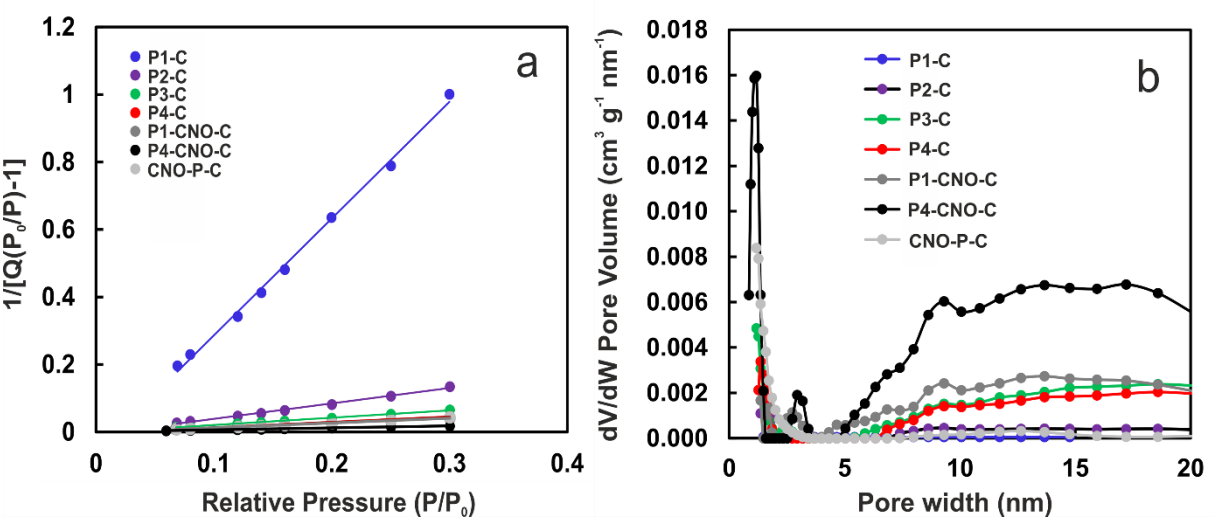

Figure S10. (a) BET curves and (b) pore volume distribution obtained for the synthesized materials from N_2 adsorption/desorption measurements.

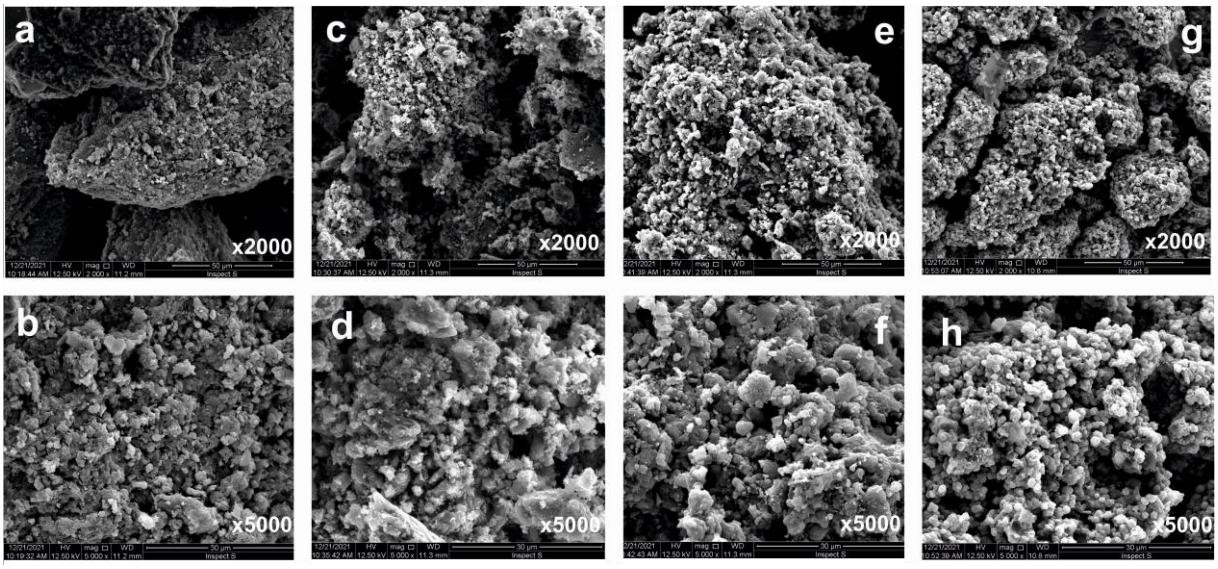

Figure S11. SEM images of polyacrylonitrile-derived block star polymers with the different chain lengths: (a, b) **P1-C**, (c, d) **P2-C**, (e, f) **P3-C**, and (g, h) **P4-C**.

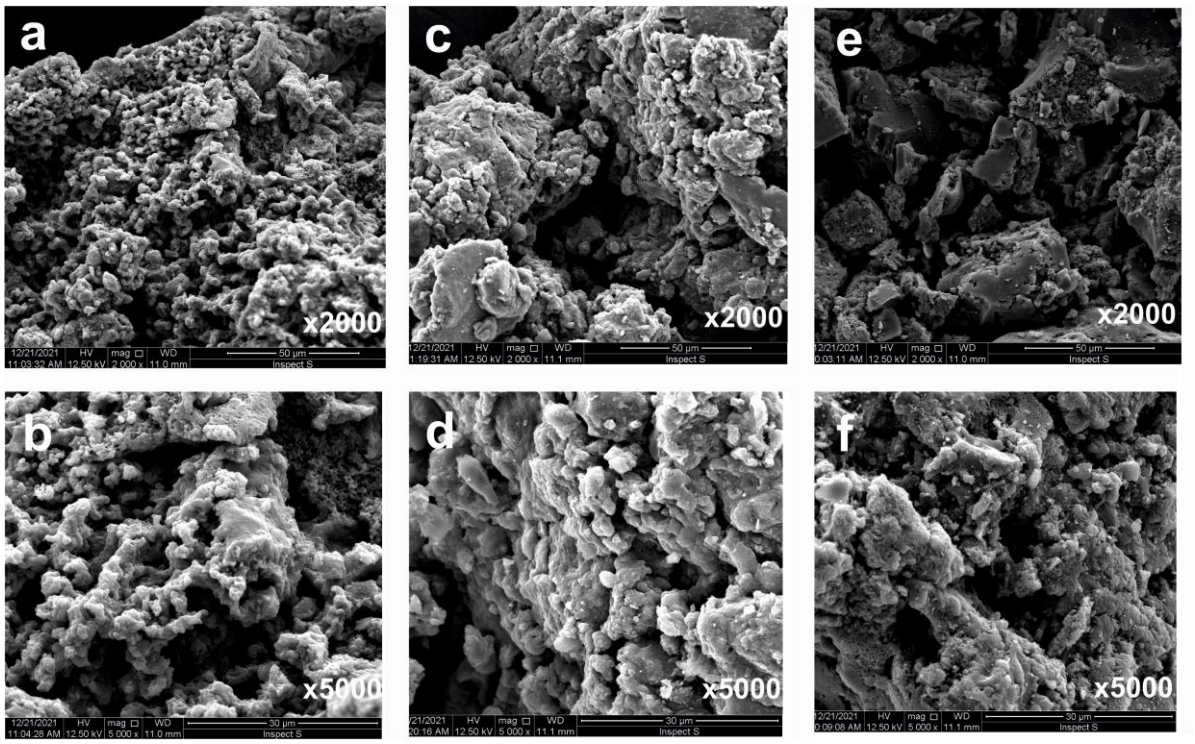

Figure S12. SEM images of polyacrylonitrile-derived block star polymer/CNO hybrids synthesized by different approaches: (a, b) **P1-CNO-C**, (c, d) **P4-CNO-C**, and (e, f) **CNO-P-C**.

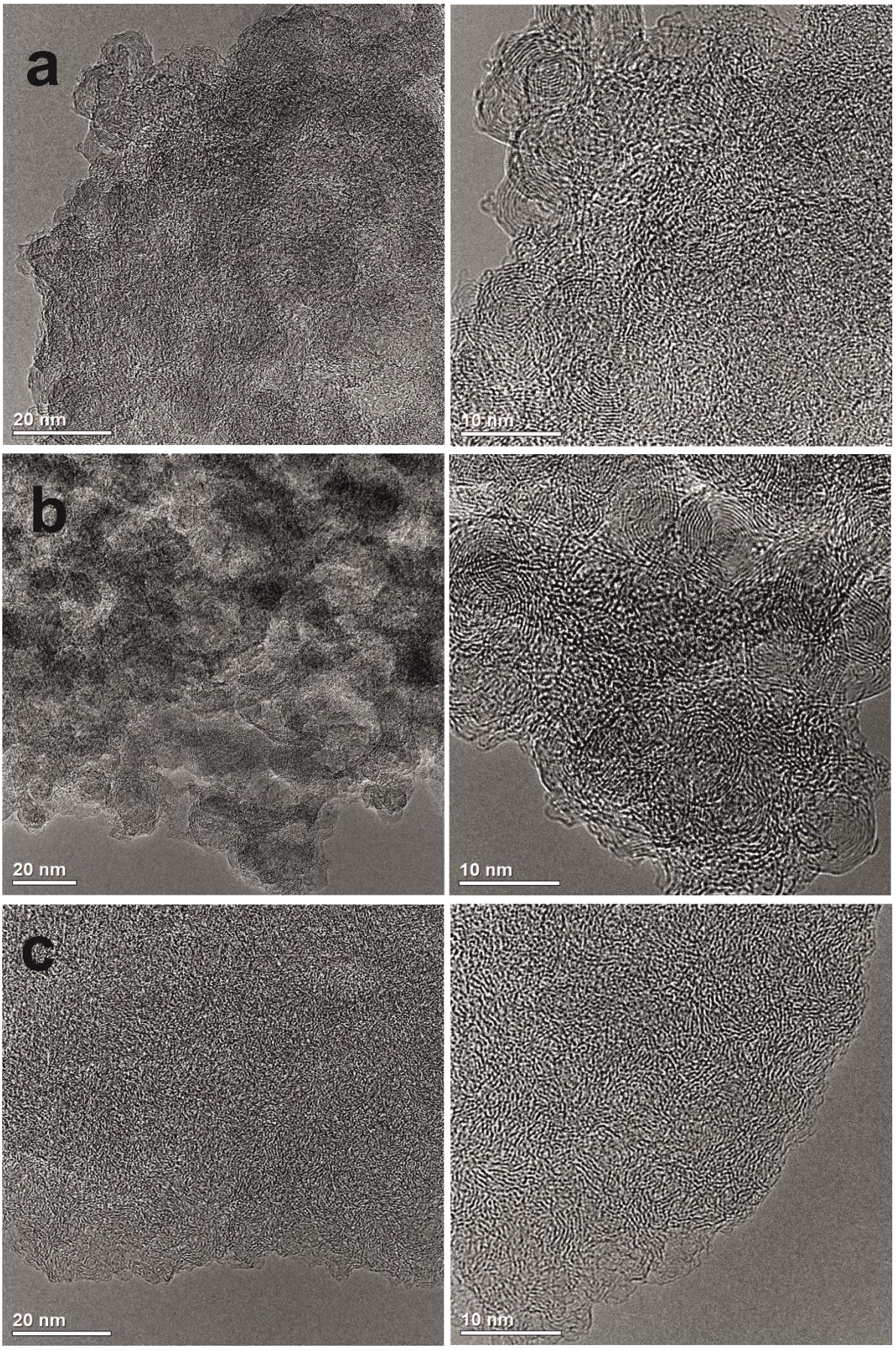

Figure S13. HRTEM images of (a) **P1-CNO-C**, (b) **P4-CNO-C**, and (c) **CNO-P-C**.

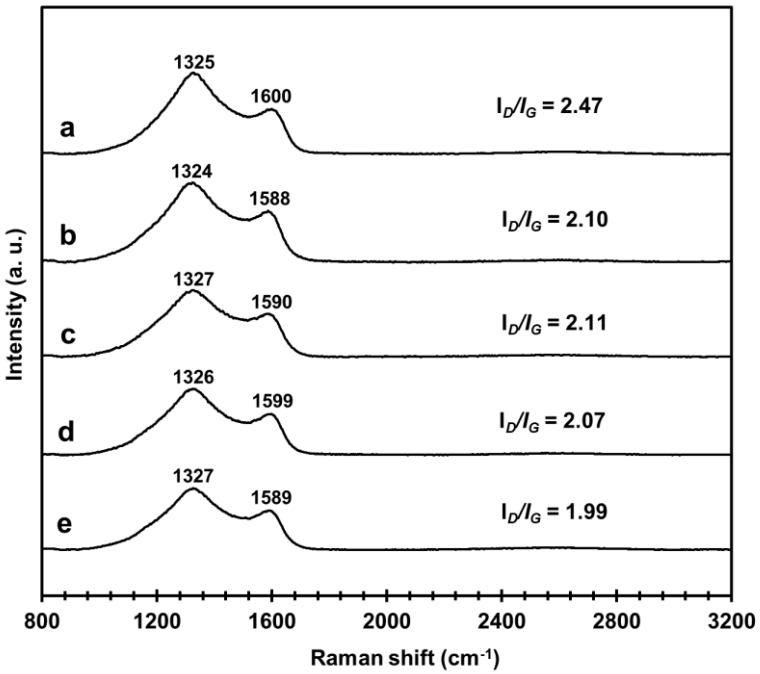

Figure S14. Raman spectra of (a) **P1-C**, (b) **P1-CNO-C**, (c) **P4-C**, (d) **P4-CNO-C**, (e) **CNO-P-C**.

All polymeric (**P1-C** and **P4-C**) and polymer-CNO hybrid materials (**P1-CNO-C**, **P4-CNO-C**, and **CNO-P-C**) after pyrolysis possess wide overlapping bands at ca. 1325 and ca. 1595 cm^{-1}, which are characteristic of the CN-disorder induced *D* band and graphitic peak *G*, respectively.[5] These vibrations are characteristic of the N-doped nanographene formed from polyacrylonitrile due to thermal stabilization and annealing.[6] Due to the overlapping of these vibrations with the *D* and *G* bands of CNOs, the presence of CNOs in the structure of hybrid material cannot be confirmed by Raman spectroscopy. Comparing the *D* to *G* intensity ratio (I_D/I_G) of the pyrolyzed polymers and the CNO−polymer hybrids, we get information about the graphitization degree of the carbons. The I_D/I_G value of polymerized polymers is always higher compared to the corresponding hybrid (*e.g.,* **P1-C** has I_D/I_G equal to 2.47 while **P1-CNO-C** has I_D/I_G equal to 2.10). The I_D/I_G value is the highest for the **P- P4-CNO-C** and **P-CNO-C** materials.

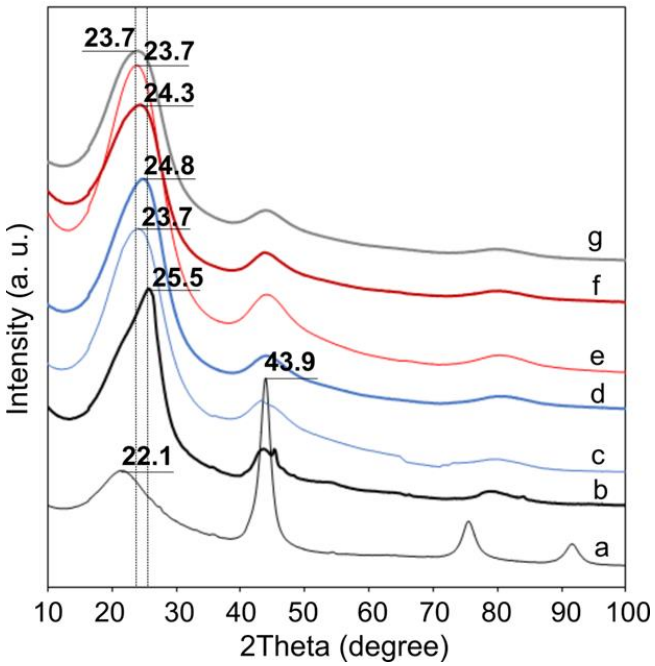

Figure S15. XRD patterns of all studied materials: (a) ND, (b) CNO, (c) **P1-C**, (d) **P1-CNO-C**, (e) **P4-C**, (f) **P4-CNO-C**, and (g) **CNO-P-C**.

The X-ray diffraction (XRD) experiments indicate the presence of various carbonaceous phases, namely diamond and graphite structures in the mesoporous carbon materials (Fig. S15). For all materials, the most substantial asymmetric peak for the 2θ angle ranging from 22 to 25° corresponds to the graphite's (002) plane,[22,23] suggesting the contribution of sp^2-bonded carbon atoms. Additionally, its asymmetry is related to two separate forms of carbon, turbostratic (amorphous) and graphene (graphitic carbon).[24] The reflex at 43.9° that is present in all materials corresponds to the (101) basal plane diffraction in the diamond structure,[25] suggesting the presence of sp^3-bonded carbon atoms.

The addition of CNOs to the polymer sample increases the crystallinity of these hybrid materials. The width of (002) peak decreases with a simultaneous increase in their height and shifts to the higher angle values, which indicates an increase in the graphitized form in the materials containing CNOs. In the pristine CNOs, the broad peak around 2θ = 25.5° is detected (Fig. S15b). It is of note that in pure polymeric samples **P1-C** and **P4-C**, homologous peak is also observed (Figs. S15c and S15e) that confirms the contribution of sp^2-bonded carbon in these materials. However, for the polymer samples this broad peak reaches its maximum at 2θ angle equal to 23.7° and 24.3° - 24.8° for the CNO composites. Moreover, the (002) reflection is sharper for **P1-CNO-C** and **P4-CNO-C** materials compared to polymer reference

samples (**P1-C** and **P4-C**), suggesting that the materials containing CNOs moiety are the graphite-like structures with a higher-order spacial arrangement.

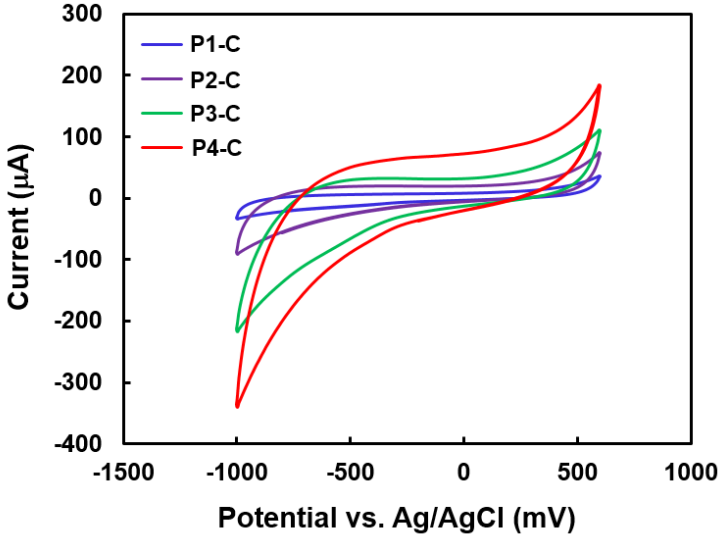

Figure S16. CVs of the GCE modified with **P1-C**, **P2-C**, **P3-C,** and **P4-C**. All voltammograms were recorded in 1 M NaOH at a scan rate of 50 mV s^{-1}.

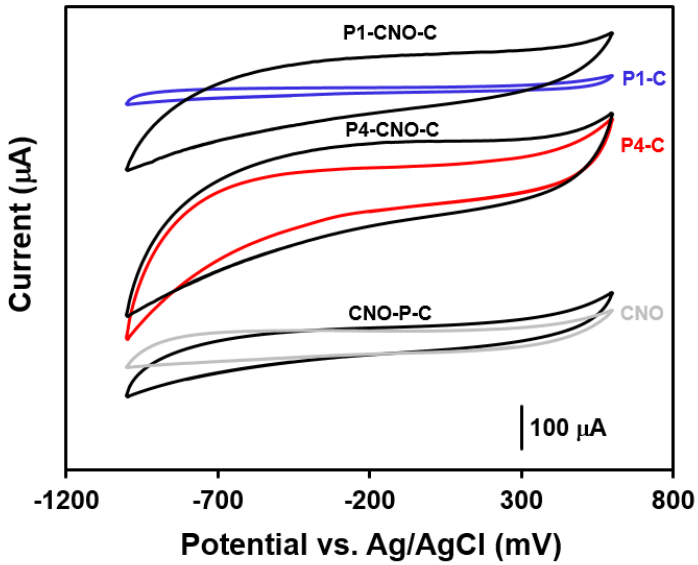

Figure S17. Comparison of the CVs recorded at the GCE modified with **P1-CNO-C**, **P4-CNO-C,** and **CNO-P-C**; the corresponding pristine polymers and CNOs were shown for the comparision. All voltammograms were recorded in 1 M NaOH at a scan rate of 50 mV s^{-1}.

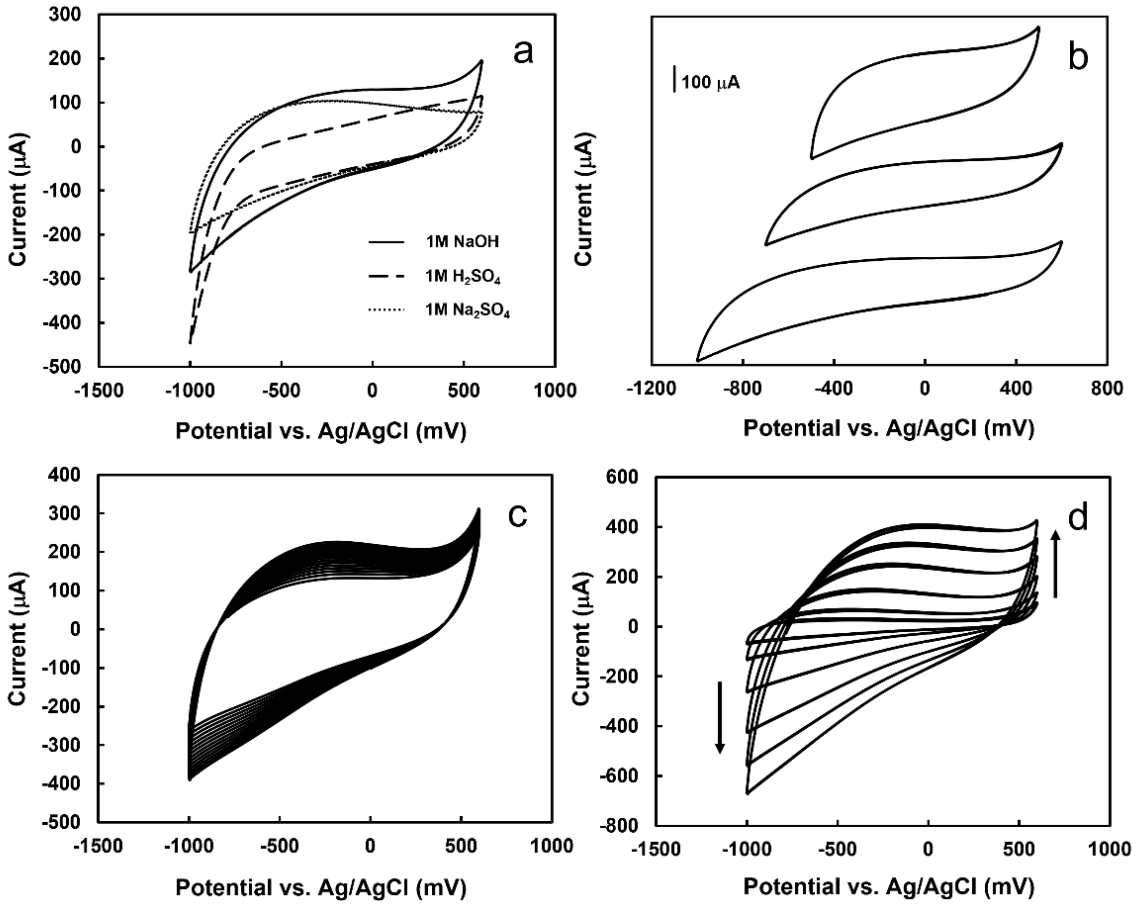

Figure S18. (a) CVs of the GCE modified with **P4-CNO-C** recorded in the different electrolytes, (b) at the different potential ranges, (c) 15 cycles, and (d) at different scan rates (from 10 to 200 mV s^{-1}). (a-c) CVs recorded at a scan rate of 50 mV s^{-1}. (b-d) CVs recorded in 1 M NaOH.

REFERENCES

1 O. Mykhailiv, H. Zubyk, K. Brzezinski, M. Gras, G. Lota, M. Gniadek, E. Romero, L. Echegoyen and M. E. Plonska-Brzezinska, *ChemNanoMat*, 2017, **3**, 583–590.

2 V. L. Kuznetsov, A. L. Chuvilin, Y. V. Butenko, I. Yu. Mal'kov and V. M. Titov, *Chem. Phys. Lett.*, 1994, **222**, 343–348.

3 A. K. Dhiman, S. S. Gupta, R. Sharma, R. Kumar and U. Sharma, *J. Org. Chem.*, 2019, **84**, 12871–12880.

4 N. Hosono, M. Gochomori, R. Matsuda, H. Sato and S. Kitagawa, *J. Am. Chem. Soc.*, 2016, **138**, 6525–6531.

5 G. Siemiaszko, A. Hryniewicka, J. Breczko, O. Fernandez Delgado, K. H. Markiewicz, L. Echegoyen and M. E. Plonska-Brzezinska, *ACS Appl. Polym. Mater.*, 2022, **4**, 2442–2458.

6 M. Koinuma, H. Tateishi, K. Hatakeyama, S. Miyamoto, C. Ogata, A. Funatsu, T. Taniguchi and Y. Matsumoto, *Chem. Lett.*, 2013, **42**, 924–926.

7 M. K. Rabchinskii, S. A. Ryzhkov, D. A. Kirilenko, N. V. Ulin, M. V. Baidakova, V. V. Shnitov, S. I. Pavlov, R. G. Chumakov, D. Yu. Stolyarova, N. A. Besedina, A. V. Shvidchenko, D. V. Potorochin, F. Roth, D. A. Smirnov, M. V. Gudkov, M. Brzhezinskaya, O. I. Lebedev, V. P. Melnikov and P. N. Brunkov, *Sci. Rep.*, 2020, **10**, 6902.
8 S. K. Ujjain, R. Bhatia and P. Ahuja, *J. Saudi Chem. Soc.*, 2019, **23**, 655–665.
9 G. Radaelli, J. A. Heredia-Guerrero, M. T. Masood, L. Ceseracciu, A. Davis, R. Carzino, M. Prato, I. S. Bayer and A. Athanassiou, *Adv. Mater. Interfaces*, 2016, **3**, 1600069.
10 H. Xu, B. Yang, J. Wang, S. Guang and C. Li, *Macromolecules*, 2005, **38**, 10455–10460.
11 Y.-C. Chiang, Y.-J. Chen and C.-Y. Wu, *Materials*, 2017, **10**, 1296.
12 A. Barinov, O. B. Malcioğlu, S. Fabris, T. Sun, L. Gregoratti, M. Dalmiglio and M. Kiskinova, *J. Phys. Chem. C*, 2009, **113**, 9009–9013.
13 R. Arrigo, M. Hävecker, S. Wrabetz, R. Blume, M. Lerch, J. McGregor, E. P. J. Parrott, J. A. Zeitler, L. F. Gladden, A. Knop-Gericke, R. Schlögl and D. S. Su, *J. Am. Chem. Soc.*, 2010, **132**, 9616–9630.
14 N. K. Gupta, B. Peng, G. L. Haller, E. E. Ember and J. A. Lercher, *ACS Catal.*, 2016, **6**, 5843–5855.
15 G. Tuci, L. Luconi, A. Rossin, E. Berretti, H. Ba, M. Innocenti, D. Yakhvarov, S. Caporali, C. Pham-Huu and G. Giambastiani, *ACS Appl. Mater. Interfaces*, 2016, **8**, 30099–30106.
16 M. Raicopol, C. Andronescu, R. Atasiei, A. Hanganu and L. Pilan, *J. Electrochem. Soc.*, 2014, **161**, G103–G113.
17 H. He, Y. Hu, S. Chen, L. Zhuang, B. Ma and Q. Wu, *Sci. Rep.*, 2017, **7**, 3913.
18 Y. J. Oh, J. J. Yoo, Y. I. Kim, J. K. Yoon, H. N. Yoon, J.-H. Kim and S. B. Park, *Electrochimica Acta*, 2014, **116**, 118–128.
19 L. Stobinski, B. Lesiak, A. Malolepszy, M. Mazurkiewicz, B. Mierzwa, J. Zemek, P. Jiricek and I. Bieloshapka, *J. Electron Spectrosc. Relat. Phenom.*, 2014, **195**, 145–154.
20 J. Baltrusaitis, C. R. Usher and V. H. Grassian, *Phys. Chem. Chem. Phys.*, 2007, **9**, 3011.
21 E. Tovar-Martinez, J. A. Moreno-Torres, J. V. Cabrera-Salazar, M. Reyes-Reyes, L. F. Chazaro-Ruiz and R. López-Sandoval, *Carbon*, 2018, **140**, 171–181.
22 S. Tomita, A. Burian, J. C. Dore, D. LeBolloch, M. Fujii and S. Hayashi, *Carbon*, 2002, **40**, 1469–1474.
23 A. E. Aleksenskii, M. V. Baidakova, A. Ya. Vul', V. Yu. Davydov and Yu. A. Pevtsova, *Phys Solid State*, 1997, **39**, 1007–1015.
24 Q.-H. Yang, P.-X. Hou, M. Unno, S. Yamauchi, R. Saito and T. Kyotani, *Nano Lett*, 2005, **5**, 2465–2469.
25 S. Tomita, M. Fujii and S. Hayashi, *Phys Rev B*, 2002, **66**, 245424.